46th AIAA/ASME/ASCE/AHS/ASC Structures, Structural Dynamics & Materials Conference,
Austin, Texas, 18-21 April 2005.

Active Aeroelastic Control of Lifting Surfaces via Jet Reaction Limiter Control

Christina Rubillo [1], Erik Bollt[2] and Piergiovanni Marzocca[3]
Clarkson University, Potsdam, New York 13699-5725, USA

The design and modeling of a novel limiter jet reaction torquer control of a wing with potentially chaotic dynamics is the topic of this paper. This study will provide a better understanding of the nonlinear dynamics of the open/closed-loop aeroelasticity of flexible wings with either steady or unsteady aerodynamic loads. The limiter control can be applied to either the plunging or pitching characteristic of the wing or both of them. On a prototypical the control can effectively suppress Limit Cycle Oscillations (LCO) and chaos well beyond the nominal flutter speed. This could lead to a practical implementation of the control mechanism on actual and future generation aircraft wings via implementation of a combination of propulsive/jet type forces, micro surface effectors, and fluidic devices. Analysis of this control produced favorable results in the suppression of LCO amplitude and increased flutter boundaries for plunging and pitching motion. The dynamic limiting control has asymptotically zero power and is simply implemented making it a feasible solution to the problem of the chaotic dynamics of the oscillating airfoil.

Nomenclature

a = Dimensionless elastic axis position measured from the midchord, positive aft
b = Half-chord length
$C_{L\alpha}$ = Lift-curve slope
ε = Nonlinear stiffness factor
$g_{h,}\, g_{\alpha}$ = Plunging and pitching control gain, respectively
h, α = Plunging displacement and the twist angle about the pitch axis, respectively
$K_{h,}\, K_{\alpha}$ = Spring stiffness in plunge and pitch directions, respectively
m = Airfoil mass per unit span
$Q_{c,h}\, Q_{c,\alpha}$ = Plunge and pitch control respectively
$Q_{h,}\, Q_{\alpha}$ = Aerodynamic lift and moment, respectively
r_{α} = Non-dimensional radius of gyration about elastic axis (EA)
t, τ_0, τ = Time variables and dimensionless time, $(\equiv tU/b)$
U = Free-stream speed
U_F = Flutter Speed
x_{α} = Non-dimensional static unbalance of the airfoil about its elastic axis; CG-EA offset
$\delta_{h,}\, \delta_{\alpha}$ = Plunging and pitching control perturbation
ζ_h, ζ_{α} = Damping coefficients in plunging and pitching
ζ = $\zeta_h/(\pi\rho b^4\omega_{\alpha}) = \zeta_{\alpha}/(\pi\rho b^4\omega_{\alpha})$ = non-dimensional damping coefficient
$\phi(\tau)$ = Wagner indicial function in the time domain
μ = $m/\pi\rho b^2$, airfoil-to-air mass ratio
ρ = Air density
$\omega_{h,}\, \omega_{\alpha,}$ = Uncoupled natural frequency in bending and torsion respectively

[1] Graduate Student, Department of Mechanical and Aeronautical Engineering, Member AIAA.
[2] Associate Professor, Department of Mathematics and Computer Sciences and Department of Physics.
[3] Assistant Professor, Department of Mechanical and Aeronautical Engineering, Member AIAA.

$\overline{\omega}$ = Frequency ratio, ω_h / ω_α

$(\dot{})$ = d( )/dτ, differentiation with respect to the non-dimensional time τ

I. Introduction

The tendency to reduce weight, increase structural flexibility and operating speed certainly increases the likelihood of the flutter occurrence within the aircraft operational envelope. Moreover, combat aircraft can experience, during their operational life, dramatic reductions of the flutter speed that can affect their survivability [1-6]. The mission profile of the next generation of UAV will probably lead to a configuration requirement of an adaptable airframe to best meet the varying flight conditions. It is conceivable that the changes in geometry that occur would also incur aeroelastic instabilities, such as flutter, at points of transition during the mission.

Conventional methods of examining aeroelastic behavior have relied on a *linear approximation* of the governing equations of the flowfield and the structure. However, aerospace systems inherently contain *structural* and *aerodynamic nonlinearities* [7] and it is well known that with these nonlinearities present, an aeroelastic system may exhibit a variety of responses that are typically associated with nonlinear regimes of response, including Limit Cycle Oscillation (LCO), flutter, and even chaotic vibrations [8]. These nonlinearities result from unsteady aerodynamic sources, such as in transonic flow condition or at high angle of attack, large deflections, and partial loss of structural or control integrity. Aeroelastic nonlinearities have been identified in [9] and analyses, focusing on LCO behavior and flutter boundaries, have been performed on similar airfoils, as well as aeroelastic panels [10-13]. Previous work has shown that airfoils operating past the flutter boundary produce LCO that increase in amplitude with increased speed, limiting the safe flight boundary [14].

The interest toward the development and implementation of active control technology was prompted by the new and sometimes contradictory requirements imposed on the design of the new generation of the flight vehicle that mandated increasing structural flexibilities, high maneuverability, and at the same time, the ability to operate safely in severe environmental conditions. In the last two decades, the advances of active control technology have rendered the applications of active flutter suppression and active vibrations control systems feasible [15, 16]. A great deal of research activity devoted to the aeroelastic active control and flutter suppression of flight vehicles has been accomplished. The state-of-the-art advances in these areas are presented in [17, 18]. The reader is also referred to a sequence of articles [19] where a number of recent contributions related to the active control of aircraft wing are discussed at length.

Early studies have shown that the flutter instability can be postponed and consequently the flight envelope can be expanded via implementation of a *linear feedback control* capability. However, the conversion of the catastrophic type of flutter boundary into a benign one requires the incorporation of a *nonlinear feedback* capability given a nonlinear aeroelastic system. In recent years, several active linear and nonlinear control capabilities have been implemented. Digital adaptive control of a linear aeroservoelastic model [20], μ-method for robust aeroservoelastic stability analysis [21], gain scheduled controllers [22], neural and adaptive control of transonic wind-tunnel model [23, 24] are only few of the latest developed active control methods. Linear control theory, feedback linearizing technique, and adaptive control strategies have been derived to account for the effect of nonlinear structural stiffness [25, 26]. A model reference variable structure adaptive control system for plunge displacement and pitch angle control has been designed using bounds on uncertain functions, [27]. This approach yields a high gain feedback discontinuous control system. In [28], an adaptive design method for flutter suppression has been adopted while utilizing measurements of both the pitching and plunging variables.

This paper will present a simple and yet effective limiter jet reaction torquer control that would enable an increase in flutter speed, enhance the aeroelastic response, and suppress LCO and chaotic dynamics, preventing catastrophic failure. The nonlinear approach of lifting surfaces of aeronautical and space vehicles permits determination of the conditions under which un-damped oscillations can occur at velocities below the flutter speed, and also of the conditions under which the flight speed can be exceeded beyond the flutter instability, without catastrophic failure, i.e. when a stable LCO takes place. The next generation of aircraft will not be mission specific, but will instead be able to adapt to many different situations and requirements, so the use of these controls to expand the safe flight boundary of an aircraft opens large opportunities in this direction. These facts emphasize the importance of at least two issues: i) various nonlinear effects should be included in the aeroelastic analysis; ii) implementing adequate control methodologies will enable one to expand the flight envelope by increasing the flutter speed, or to enhance

the aeroelastic response by attenuating the excessive vibrations, but also to convert the unstable LCO into a stable one [29].

More insight into the wealth of the limiting dynamic control developed in [15, 30-31] and applied to this important aeroelastic problem is provided. Limiter control uses small perturbations to neutralize system instabilities. This technique has been applied to simple mechanical systems, such as a pendulum, and to electric circuits [32]. Dynamic limiting continuously adjusts the limiter value, allowing for more effective chaos control [31]. While other forms of nonlinear control of aeroelastic structural systems have previously been researched [29], the feasibility of dynamic limiting, as applied to a nonlinear airfoil, is explored in this paper. In section II, the mathematical model of the plunging/pitching airfoil will be introduced, as well as the dynamic limiting control. Section III outlines the results of the applied control on the airfoil in steady and unsteady flow, focusing on LCO suppression and flutter boundary extension. A brief summary of the conclusions can be found in section IV.

II. Mathematical Model

A classical two degrees-of-freedom in pitch and plunge airfoil will be used to evaluate the limiter control. The schematic for this system is shown in Fig.1.

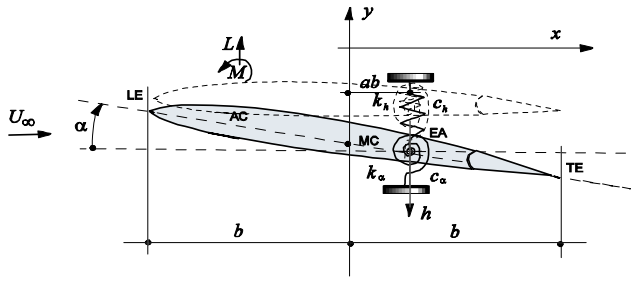

Fig. 1: 2-DOF pitching and plunging airfoil

For this model the nonlinear aeroelastic governing equations are [11]

$$\mu\ddot{h} + \mu\chi_\alpha\ddot{\alpha} + \zeta\dot{h} + \mu\left(\frac{\omega_h}{\omega_\alpha}\right)^2 h = -\frac{Q_h}{\pi\rho b^3 \omega_\alpha{}^2} \tag{1}$$

$$\mu\chi_\alpha\ddot{h} + \mu r_\alpha{}^2\ddot{\alpha} + \zeta\dot{\alpha} + \mu r_\alpha{}^2\alpha + \frac{\varepsilon}{\pi\rho b^4 \omega_\alpha{}^2}\alpha^3 = \frac{Q_\alpha}{\pi\rho b^4 \omega_\alpha{}^2} \tag{2}$$

where h and α are the plunge and pitching angle displacement. In addition to the well known structural terms, see [1-4], the aerodynamic lift and moment forces are represented by Q_h, Q_α, respectively.
A model with unsteady aerodynamics will also be considered. The lift and moment are expressed as[33]:

$$Q_h(\tau) = -C_{L\alpha} b\rho U^2 \int_{-\infty}^{\tau} \phi(\tau - \tau_0)\left[\dot{\alpha} + \frac{\ddot{h}}{b} + \left(\frac{1}{2} - a\right)\ddot{\alpha}\right] d\tau_0 - \frac{1}{2}\rho C_{L\alpha} U^2\left(\ddot{h} - ab\ddot{\alpha}\right) - \frac{1}{2}\rho C_{L\alpha} b U^2 \dot{\alpha} \tag{3}$$

$$Q_\alpha(\tau) = \left(\frac{1}{2} + a\right) C_{L\alpha} b^2 \rho U^2 \int_{-\infty}^{\tau} \phi(\tau - \tau_0)\left[\dot{\alpha} + \frac{\ddot{h}}{b} + \left(\frac{1}{2} - a\right)\ddot{\alpha}\right] d\tau_0 + \frac{1}{2} ab\rho C_{L\alpha} U^2\left(\ddot{h} - ab\ddot{\alpha}\right) - \frac{1}{2}\left(\frac{1}{2} - a\right)\rho C_{L\alpha} b^2 U^2 \dot{\alpha} - \frac{1}{16}\rho C_{L\alpha} b^2 U^2 \ddot{\alpha} \tag{4}$$

where $\phi(\tau)$ is the Wagner function. This function is best approximated with:

$$\phi(\tau) = A_1 e^{-b_1\tau} - A_2 e^{-b_2\tau} \tag{5}$$

where A_i =(0.165; 0.335) and b_i= (0.0455; 0.300) [34]. In the next sections a steady and an unsteady model for the airfoil will be presented.

From the mathematical point of view, the nonlinear aeroelastic governing equations, (1) and (2), will be coupled with a nonlinear feedback limiter control. Such control can stabilize desired orbits [35], and in this paper it is implemented toward suppressing LCO and chaotic motions. This technique has already been successfully applied to chaotic mechanical systems [36, 37], and experiments have proved its effectiveness. The dynamic limiting technique

[36, 37] enables us to selectively control unstable periodic orbits via minimal perturbations. Furthermore, recent results [37] have further extended the limiter control to allow for low-energy control in electronic devices. The jet reaction torquer/morphing control can be mathematically described via a simple state dependent, but otherwise constant addition to the uncontrolled aeroelastic system, written in general multivariable form as:

$$\dot{\mathbf{z}} = \mathbf{F}(\mathbf{z},\mathbf{p}) + \mathbf{G}(\mathbf{z},t) \tag{6}$$

where $\dot{\mathbf{z}} = \mathbf{F}(\mathbf{z},\mathbf{p})$ represents the dynamics of the uncontrolled aeroelastic system. $\mathbf{G}(\mathbf{z},t)$ represents the constant addition to the unperturbed dynamics and may be posed as combination of characteristics (indicator) functions, both spatially and temporally:

$$\mathbf{G}(\mathbf{z},t) = \sum_{n=0}^{\infty}\sum_{i=1}^{N} d_{n,i}\chi_{t_n}(t)\chi_{A_i}(\mathbf{z})\mathbf{k}_i . \tag{7}$$

For each fixed i, $d_{n,i}$ is a time independent coefficient, and χ_{t_n} and χ_{A_i} are characteristic (indicator) functions of time and space respectively. χ_{t_n} and χ_{A_i} are described as:

$$\chi_{t_n}(t) = \begin{cases} 1 & if \;\; t_n \le t \le t_{n+1} \\ 0 & else \end{cases} \tag{8}$$

$$\chi_{Ai}(t) = \begin{cases} 1 & if \;\; t \in A_i \\ 0 & else \end{cases} \tag{9}$$

Where A_i represents a region and the variable $\mathbf{k}_i$ is a constant vector addition, or direction the force should be applied, to the vectorfield whose influence tends to push the LCO in the general direction of $\mathbf{k}_i$. This should be chosen appropriately to suppress the LCO and chaotic motions. This concept is demonstrated in Fig. 2.

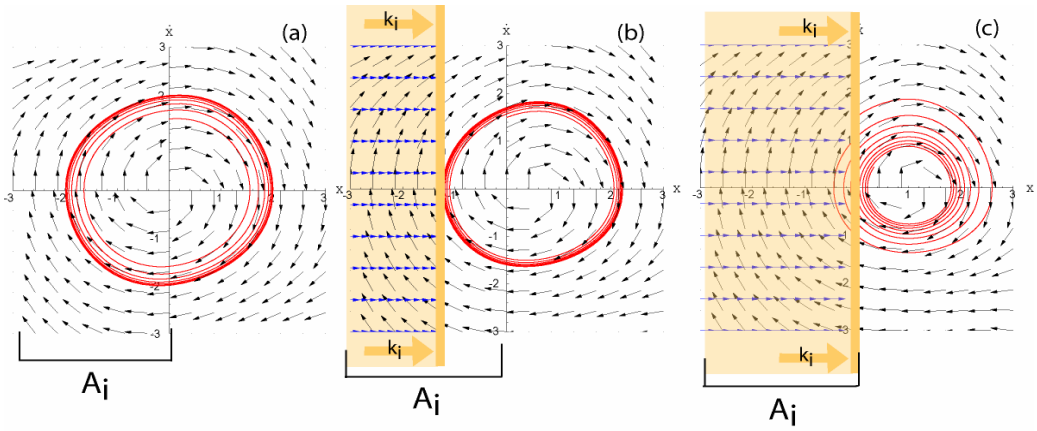

Fig. 2: Position versus velocity plot of a simple limit cycle (a) without control, (b) with a control value, $\mathbf{k}_i$, that decreases the LCO amplitude, (c) with a control value that completely damps-out the system. The shaded area represents the direction of the control value $\mathbf{k}_i$ and the magnitude of **G(z, t)** . A_i represents the region for which the control is applied.

A qualitative explanation of this control is that when the dynamics of the system enter the region, A_i, for example when the airfoil reaches a pre-defined deflection limit, the control is applied to push it back to that limit.

For the form of the limiter control mechanism, shown below for both plunging and pitching, we choose

$$Q_{c,h} = g_h H(h - \delta_h) \tag{10}$$

$$Q_{c,\alpha} = g_\alpha H(\alpha - \delta_\alpha) \tag{11}$$

This form of the control is applied in equations (12) and (13). In other words the characteristic functions in equation (7) are simplified here as the Heavyside function, H. The control gain, or direction of the pushing force, is represented by g_h and g_α, while the control perturbation is given as δ_h and δ_α. For this model the control gain can be either positive or negative since the force addition can come from either direction. When applied to the corresponding plunge or pitch governing equation this control produces the desired vector addition. Some explanatory cases will be presented in the next section for the 2-D wing model first controlling the plunging characteristics, followed by the pitching for both steady and unsteady models. Both models governing equations were numerically solved using a combination of a non-stiff Adams method and a stiff Gear method.

III. Results and Discussion

Steady Model

A linear model of the airfoil in steady flow will be analyzed first .The following parameters were used: μ =12.8, b=0.118, ζ=0.2, ω_h= 34.6, ω_α=88, r_α^2=0.3, ε = 20 and χ_α = 0.15, from [11]. For the steady flow the governing equations become:

$$12.8\ddot{h} + 1.92\ddot{\alpha} + 0.2\dot{h} + 1.97h = -\frac{1}{\pi}\left(\frac{U}{b\omega_\alpha}\right)^2 (5.568\alpha + 0.0942) + Q_{C,h} \tag{12}$$

$$1.92\ddot{h} + 3.84\ddot{\alpha} + 1.2\dot{\alpha} + 3.84\alpha + 4.24\alpha^3 = \frac{1}{\pi}\left(\frac{U}{b\omega_\alpha}\right)^2 (1.4845\alpha + 0.0084) + Q_{C,\alpha} \tag{13}$$

Fig. 3 shows the phase portraits for the steady model before and after flutter speed. For the steady model the flutter speed was found to be 17.22 m/s, which is consistent with the value obtained by [11]. These phase portraits show that after flutter speed a limit cycle is reached, with amplitude of 0.17 radians for pitching, and a maximum of 0.5 for plunging.

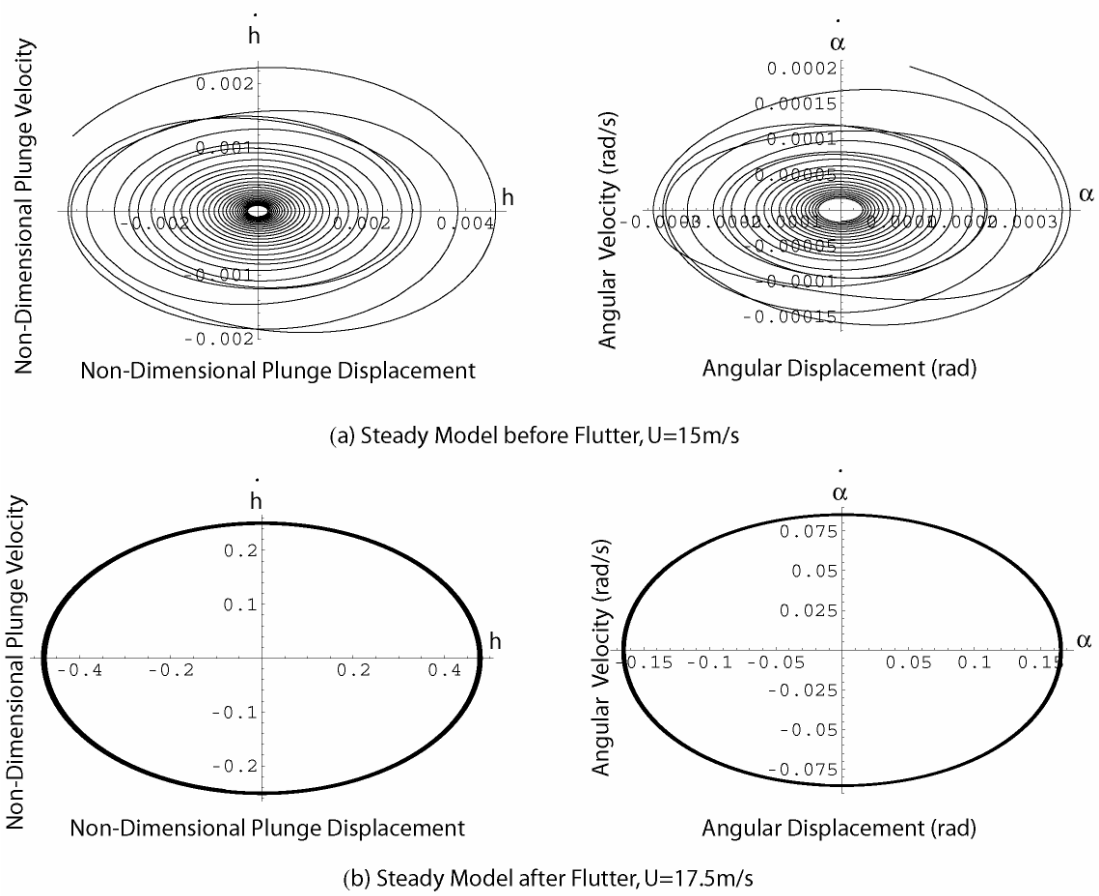

Fig.3: Phase plots depicting the LCO of the airfoil under steady flow conditions: (a) before flutter, converging to zero, U=15m/s, (b) after flutter with LCO behavior, U=17.5m/s

Before we applied any control, we analyzed the effect of the nonlinear stiffness factor, ε, on LCO amplitude. As shown in Fig. 4 increasing this stiffness factor significantly decreases the LCO amplitude, while the flutter speed remains constant. As a limiting case, ε =0, a straight vertical line at the flutter speed will be obtained. We also explored the effect of the airfoil-to-air mass ratio, μ. In Fig. 5, it is apparent that as μ increases, the LCO amplitude decreases and the flutter boundary is enhanced.

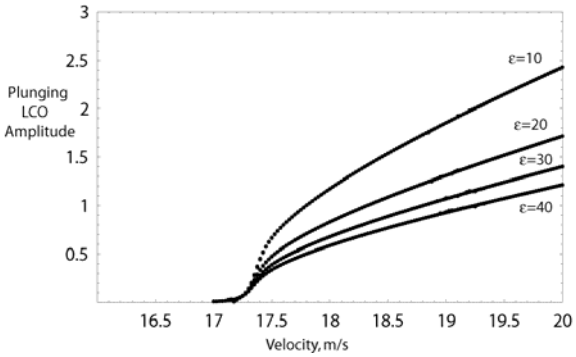

Fig. 4: Velocity versus LCO amplitude for various nonlinear stiffness factors, ε.

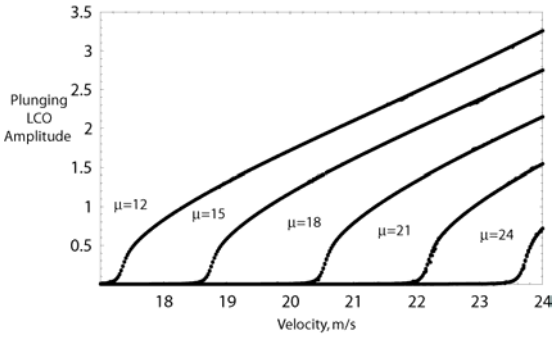

Fig. 5: Velocity versus LCO amplitude for various airfoil-to-air mass ratios, μ.

The natural uncoupled frequencies in bending and torsion, ω_h and ω_α, also have a significant effect on the flutter speed and LCO amplitude. In Fig. 6, an increase in ω_h will decrease the flutter speed and increase the LCO amplitude. The opposite is valid for ω_α, as seen in Fig. 7. Increasing the natural pitching frequency will decrease the LCO and increase the flutter boundary.

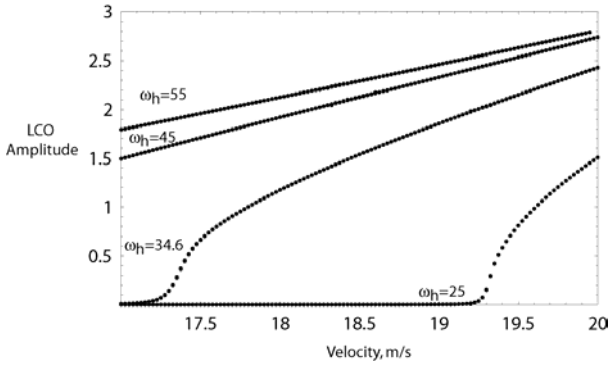

Fig. 6: Velocity versus LCO amplitude for various natural frequencies in bending, ω_h.

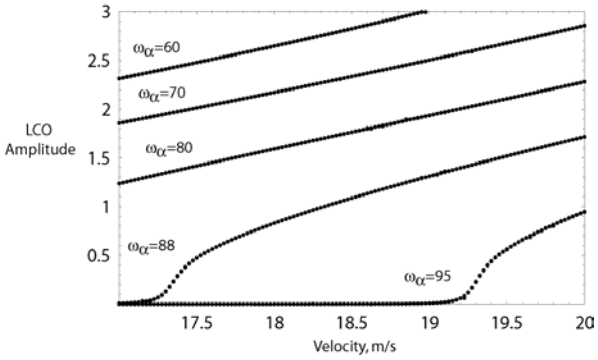

Fig. 7: Velocity versus LCO amplitude for various natural frequencies in torsion, ω_α.

Varying the radius of gyration, r_α, for the prototypical airfoil may also assist in LCO suppression and flutter boundary extension. Increasing the value of r_α extends the flutter speed and suppresses the LCO amplitude. For, r_α larger than 0.4, the LCO may only occur at very large flight speeds. χ_α represents the non-dimensional static unbalance of the airfoil, about the elastic axis, or the CG-EA offset. Increasing this parameter decreases the flutter speed and increases the LCO amplitude. As χ_α approaches 0.2, a constant LCO amplitude curve is reached for all higher offset values. For values lower than $\chi_\alpha = 0.1$, the LCO only occurs at high speeds. Although these are just parametric studies, they can give a good understanding of the post-flutter behavior, which may be characteristic of the system.

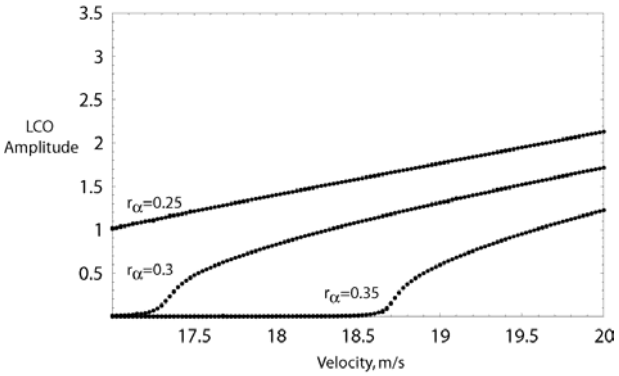

Fig. 8: Velocity versus LCO amplitude for various radii of gyration, r_α.

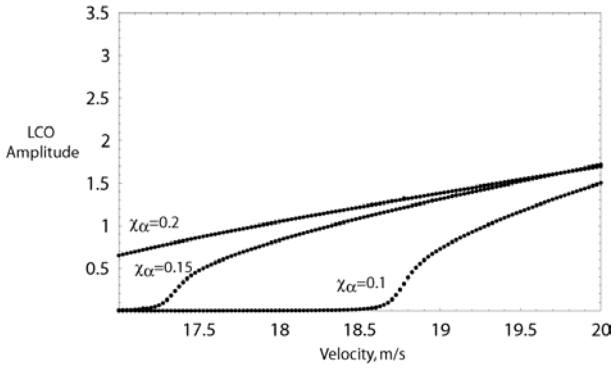

Fig. 9: Velocity versus LCO amplitude for various CG-EA offsets, χ_α.

Analysis of the steady model's flutter speed behavior, under plunge control, shows no significant change. As the control gain, g_h, and the control perturbation, δ_h, vary, the flutter speed remains constant at its uncontrolled value. Under pitch control, a considerable change in flutter speed is observed. The potential of *pitch control* in the steady model is highlighted in Fig.10. The amplitude of the LCO vs. the free stream velocity for a Plunging/Pitching airfoil with a freeplay structural non-linearity in pitch, subjected to an incompressible flow is presented. When this airfoil's flutter speed U_F is exceeded, the airfoil experiences a stable LCO and a chaotic behavior. This analysis shows that *the limiter control is capable of suppressing LCO and also the chaotic dynamics* of such an airfoil, even well beyond the flutter speed. Notice the Hopf bifurcation that occurs at flutter speed, U_F. Before this point the system is converging, however above flutter speed a stable LCO appears. At approximately U=25, the system becomes chaotic as shown in the magnified red region. The plots shown in green represent the system with the applied control. The stable limit cycle is now converging and the chaotic region has also been suppressed.

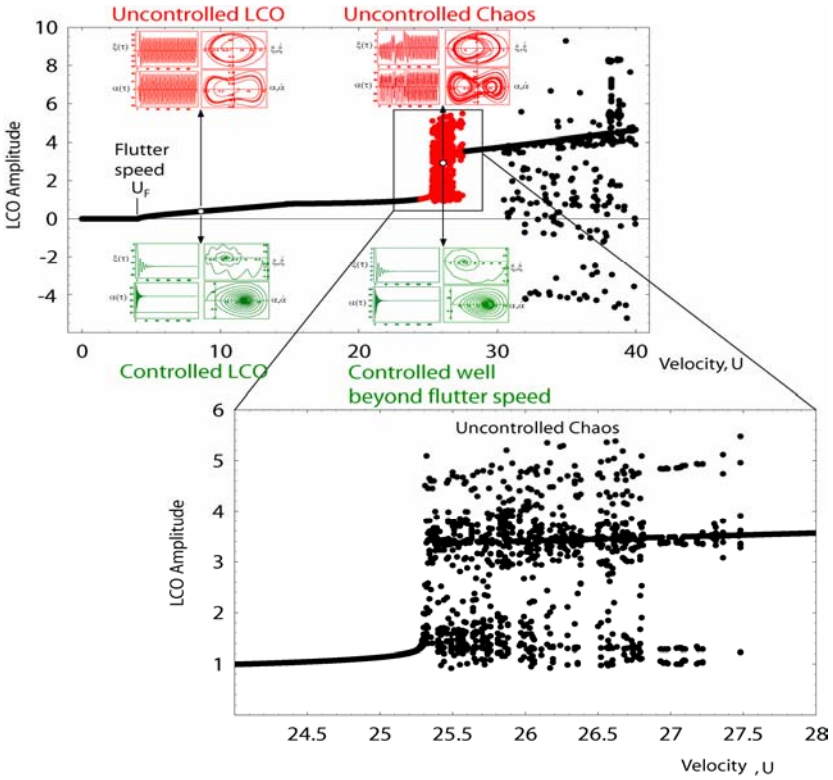

Fig. 10: LCO amplitude versus free stream velocity for a 2-DOF system. U_F represents the flutter speed, after which a stable LCO appears. After approximately U=25, a chaotic region exists. The red and green phase portraits and time histories represent the uncontrolled and controlled system, respectively.

Subjecting the steady airfoil model to pitch control at a velocity close to flutter speed can significantly damp out the system. In Fig. 11, the pitching phase portrait and time history are shown for a velocity of 17.3 m/s with and without control. The uncontrolled airfoil slowly approaches a limit cycle. The time history displays the amplitude of vibration shortly before reaches the LCO (approximately at τ =1800) and including the LCO. By applying pitch control g_α=-1, the oscillations stop before τ = 350 (2.3 seconds).

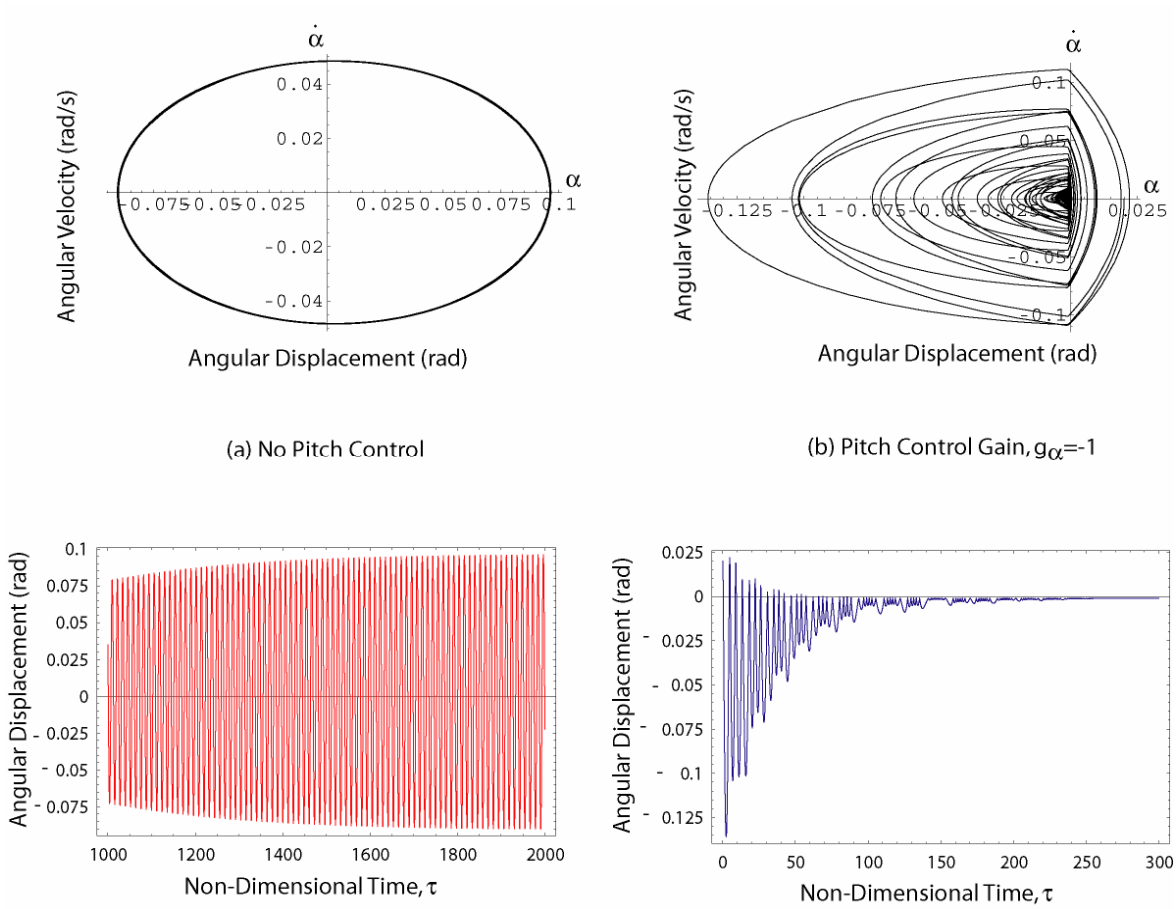

Fig. 11: Phase portraits and time histories of airfoil at U=17.3m/s (a) without control, (b) with pitching control gain, g_α=- 1, δ_α=0.001, showing that pitch control can damp the oscillating airfoil.

Flutter Analysis

The effect of pitching control gain, g_α, and control perturbation, δ_α, on flutter speed is shown in Fig. 12. This effect is very complex, but there exist combinations of g_α and δ_α, for which the control is most effective in extending the flutter boundary. One can see that, as the magnitude of the control gain increases in the negative direction, the flutter speed boundary is extended. As the magnitude of the control gain increases in the positive direction, the opposite behavior is observed. Focusing on the larger range, it is apparent that for gains larger than 0.1, the flutter speed will gradually drift to the uncontrolled flutter speed and then continually decline. In the negative direction, any gain with a magnitude larger than 0.1 decreases the flutter speed, while gains between 0 and -0.1 produce a useful increase in the flutter speed.

Fig. 12 also shows the behavior of the flutter speed as we vary the control perturbation, δ_α. Focusing primarily on the left hand side of the graph, one can observe that the lowest value of δ_α, produces the most valuable result. The flutter speed is greatly increased in the smaller control gain magnitude range. For larger perturbations the flutter speed is not improved, but decreased, further limiting the safe flight boundary. Perturbations larger than 0.05 produce flutter speed that is equivalent to the value of the uncontrolled boundary. Since δ_α is a perturbation to the angle of attack, its value should remain small and on the order of magnitude of the existing angle. From a design

perspective, this analysis will guide engineers toward selecting appropriate ranges of g_α and δ_α, for maximum performance.

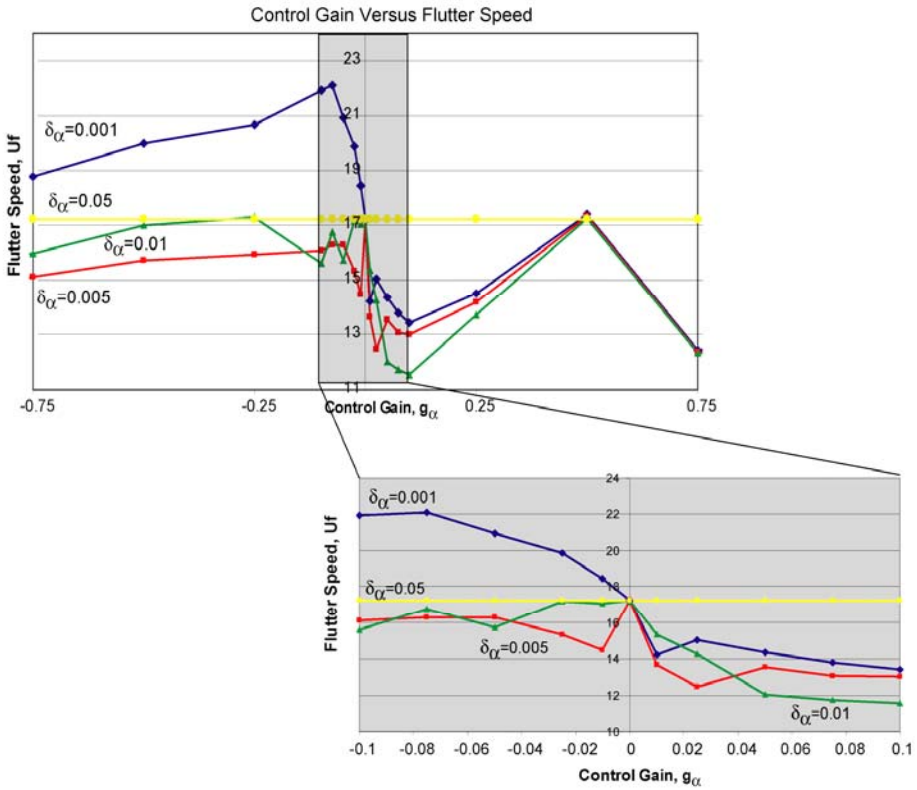

Fig. 12: Control gain, g_α, versus flutter speed for an airfoil under steady conditions with pitch control and various control perturbations.

LCO Amplitude Analysis

The Limit Cycle Oscillation amplitude of the steady model was also examined under both plunging and pitching control. Although the flutter boundary was not extended under plunge control, the LCO amplitude is slightly suppressed at lower speeds. However, for higher control gains the region before the flutter speed is unstable. Plunging control gains should be kept small for the best result in both flutter and LCO behavior. Under pitch control, the LCO amplitude is suppressed with larger control gains in the negative direction. The amplification of the LCO with larger control gains is shown in Fig. 13. After g_α=0.25 the system becomes chaotic.

The pitching control perturbation, δ_α, also contributes to LCO suppression.

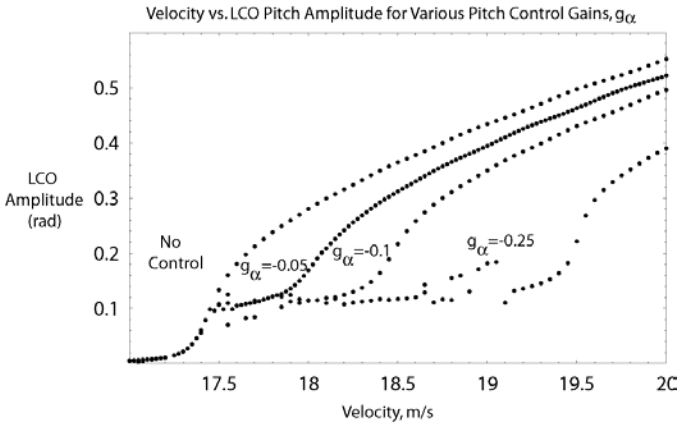

Fig 13: Free stream velocity versus LCO amplitude under pitch control. Various values of the control gain are shown, δ_α=0.001.

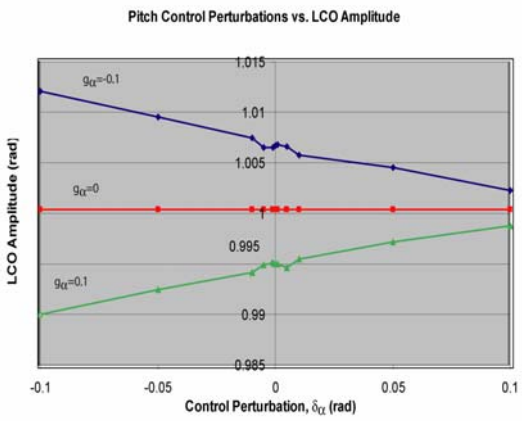

Fig. 14: Pitch control perturbations, δ_α, versus LCO Amplitude for various control gains, g_α.

Fig. 14 shows the LCO amplitude as δ_α is changed for a positive and negative control gain. Comparing this to the uncontrolled LCO, one can see that when applying a negative control gain an increase in the control perturbation in the positive directly slightly suppresses the LCO. Increasing the perturbation in the negative direction slightly amplifies the LCO. When applying a positive control gain, the opposite occurs.

Control Power Analysis

Another pertinent aspect of the limiter control presented in this paper is the power needed to maintain a stable LCO once control is applied. After control is applied the transient loops are "pushed" toward a limit cycle. The power and time plot shows how much power is required to push each transient loop to the LCO. Fig. 15 highlights the area that was observed. The points that are shown past the vertical dotted line are those where the position is less than the limit cycle. The vertical line represents the time and amplitude of the LCO.

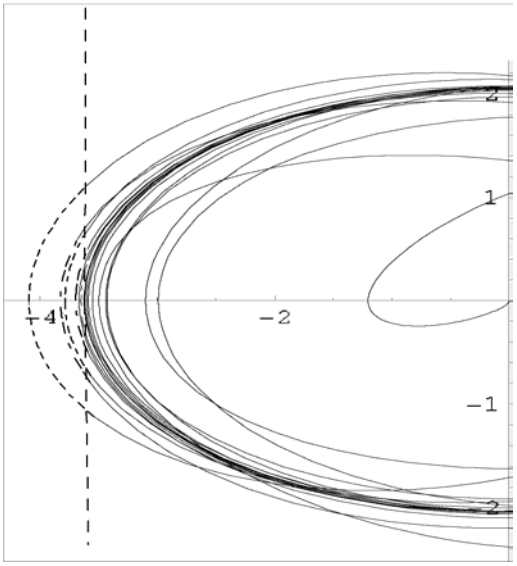

Fig. 15: Observed Region for limiter control power analysis

Fig. 16 displays a representative power plot for both plunging and pitching gains. The control gain and perturbation are small and the free stream velocity is 25m/s. Maintaining the LCO in plunge control, requires several larger power outputs with less frequency, while the pitch control needs smaller amplitude power outputs at a higher frequency. Both plots show that a relatively small amount of power is needed to maintain the smaller limit cycle. Notice that *the required power is asymptotically decreasing toward zero* as the controlled LCO is reached. Eventually the system would remain at the controlled LCO with little to no power applied.

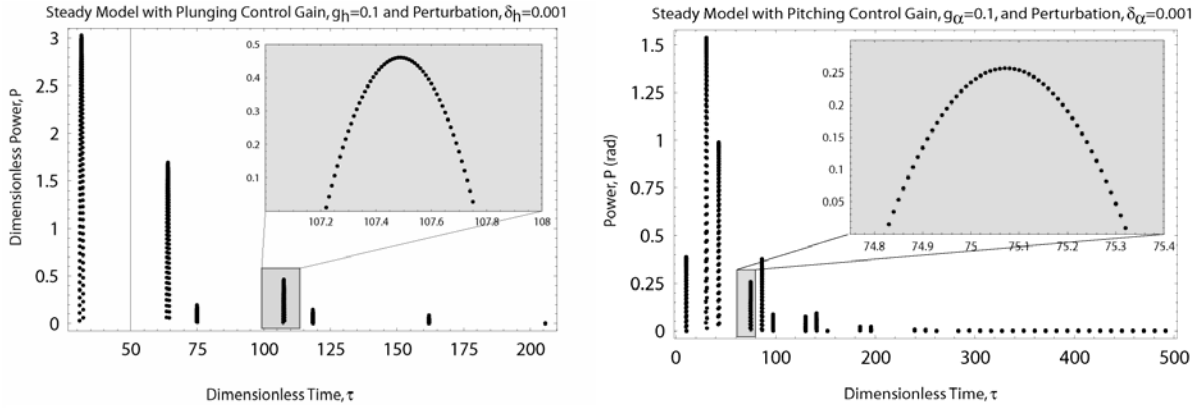

(a) (b)

Fig. 16: Power versus time for steady model with (a) plunge control, and (b) pitch control, showing that the power needed to control the LCO is asymptotically zero.

Unsteady Model

A preliminary analysis of an airfoil under unsteady flow conditions was performed. The following parameters were used: μ =13.8, b=0.118, ζ=0.2, ω_h= 34.6, ω_α=88, r_α^2=0.3, ε = 20 and χ_α = 0.15. The motion of this airfoil in plunging and pitching can be expressed as [11]:

$$13.8\ddot{h} + 2.33\ddot{\alpha} + (0.2 + 0.1926U)\dot{h} + 1.9787h + 0.2715U\dot{\alpha} + 0.01854U^2\alpha = -Q_{C,h} \qquad (14)$$

$$2.33\ddot{h} + 4.1331\ddot{\alpha} + (0.2 + 0.0718U)\dot{\alpha} + (3.84 - 0.001669U^2)\alpha + 4.24\alpha^3 - 0.01733U\dot{h} = Q_{C,\alpha} \qquad (15)$$

Fig. 17 shows the phase portraits for the unsteady model before and after flutter speed. For the unsteady model the flutter speed was found to be 19.38 m/s, this is consistent with the results obtained by [11]. These phase portraits show that after flutter speed a limit cycle is reached, with amplitude of 0.34 radians for pitching, and a maximum of 0.29 for plunging.

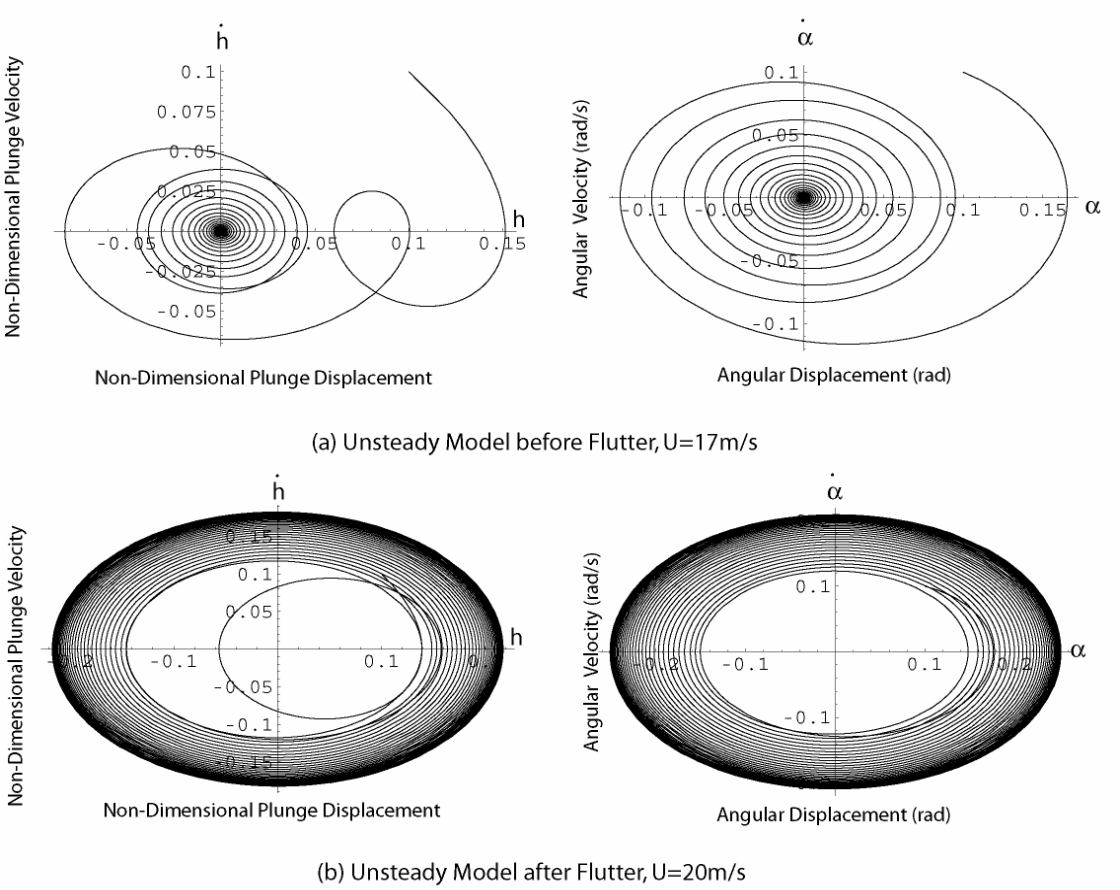

Fig. 17: Phase plots depicting the LCO of the airfoil under unsteady flow conditions: (a) before flutter, converging to zero, U=17m/s, (b) after flutter, exhibiting an LCO, U=20/s

Limiter control was placed in the plunging movement and found to have no positive effect on the flutter boundary. As the magnitude of the control gain increases in the positive direction, the flutter speed remains constant at the uncontrolled value. Increasing the plunge control perturbation produces also produces little to no change in flutter speed. *When control is applied to the pitching movement, the flutter speed is increased* with increasing gain magnitude in the negative direction. Fig. 18 exhibits the relationship between pitching control gain and flutter speed for the unsteady model, as well as the effects of control perturbation, δ_α. For δ_α values less that 0.05 the flutter curve remains constant. After 0.05 the flutter speed will always be approximately the uncontrolled value, in this case 19.38m/s. Fig. 19 shows the pitch controls influence on the LCO amplitude of the unsteady model. As the control gain is increased in the negative direction the LCO amplitude is decreased, however in the positive direction the opposite is true. As the control perturbation is increased the LCO amplitude increases with positive gain, and

decreases with negative gain. This analysis can provide a guideline for choosing appropriate perturbation-gain combinations to achieve the maximum LCO amplitude performance.

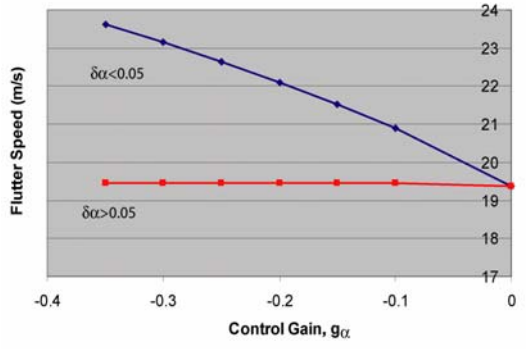

Fig. 18: Pitching control gain versus flutter speed for unsteady model

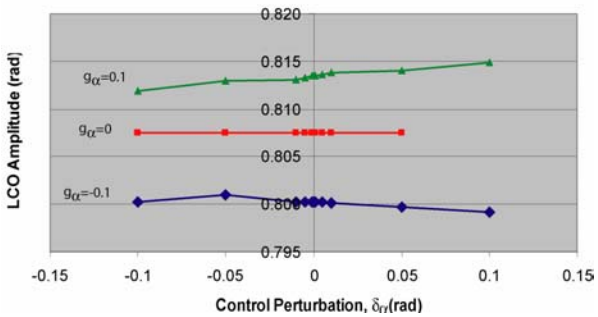

Fig. 19: Pitching control gain versus flutter speed for unsteady model

The LCO amplitude of the unsteady model can be suppressed with pitch control. Fig. 20 shows the phase portraits and time histories for a system, with a free stream velocity of U=20 m/s, which is slightly above flutter speed. With a control gain of -0.25, the vibration is completely damped.

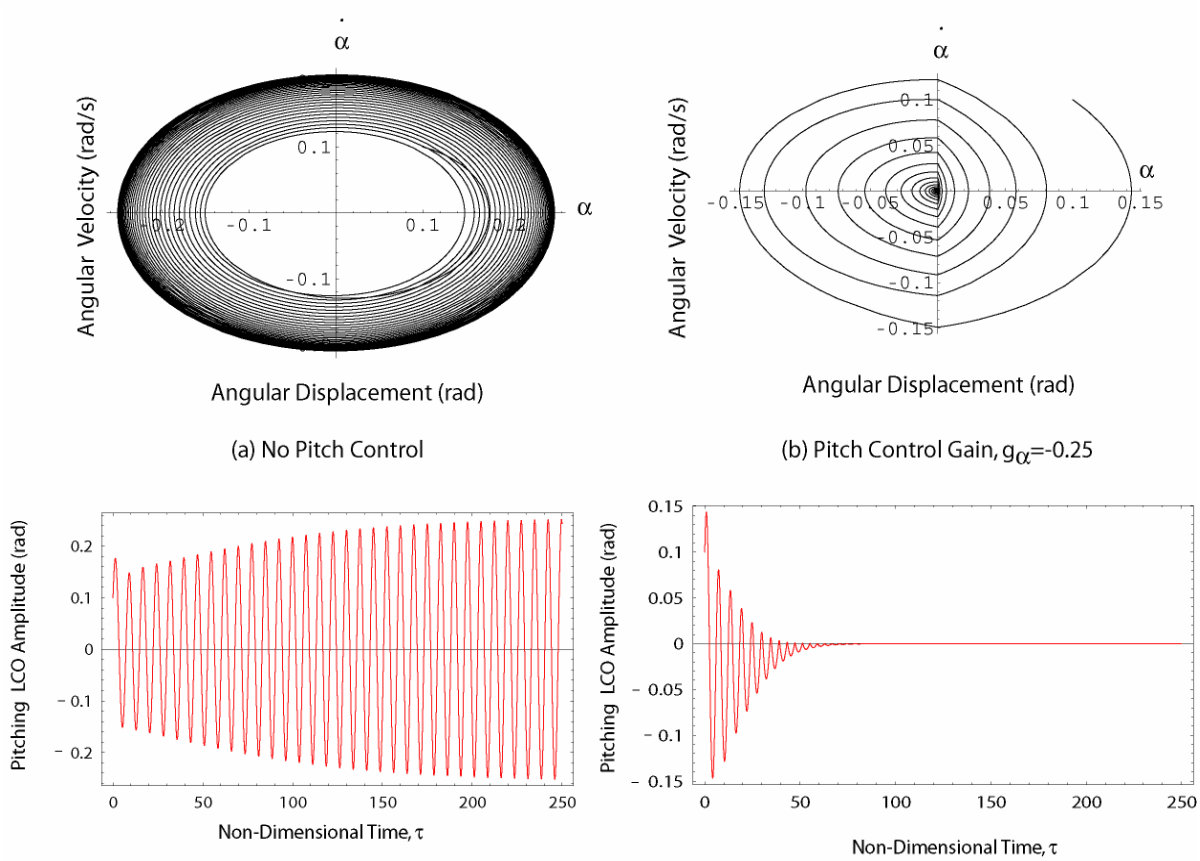

Fig. 20: Phase portraits and time histories of unsteady airfoil at U=20 m/s (a) without control, (b) with pitching control gain, g_α=-0.25, δ_α=0.001, showing that the LCO of an unsteady airfoil can be suppressed with this control.

Even before flutter speed, the dynamic limiting pitch control has a positive effect on the vibrations. A small control gain in the negative direction makes the LCO amplitude half as large. Fig. 21 shows the phase portraits before flutter, with and without control.

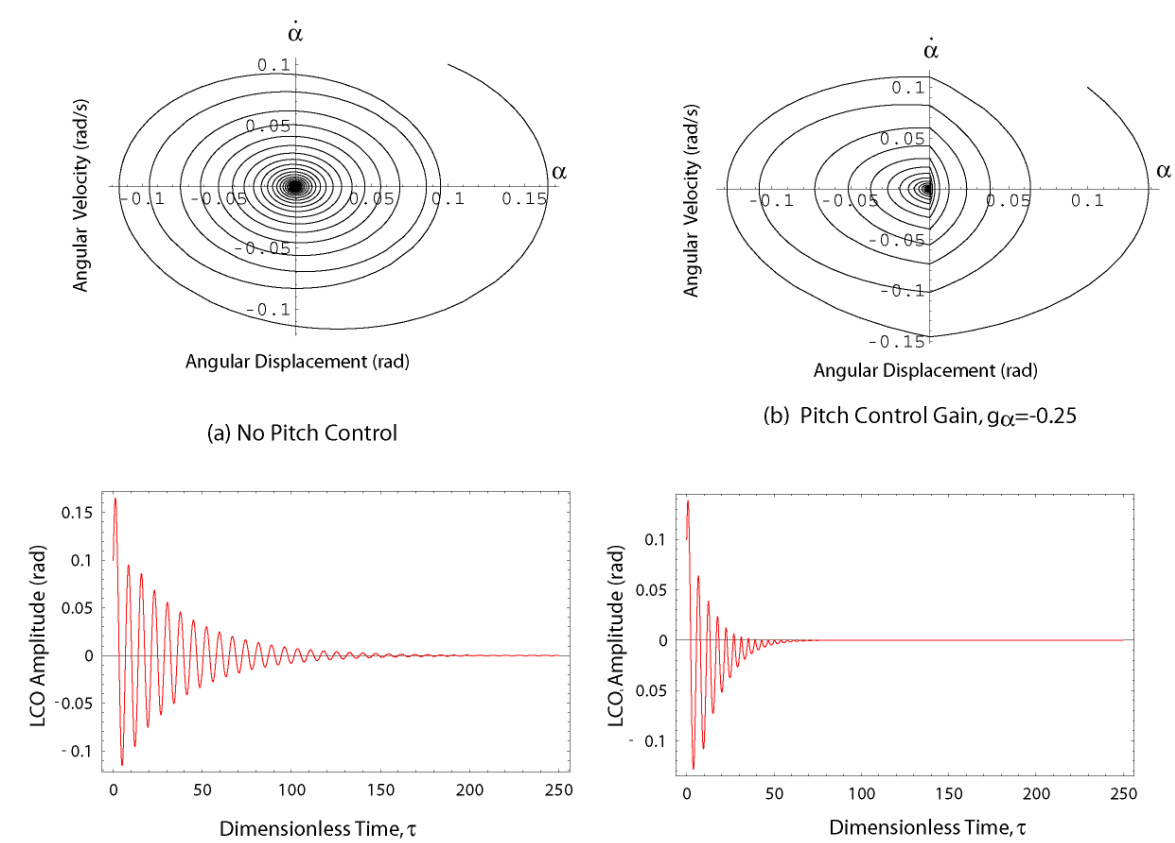

Fig. 21: Phase portraits and time histories of unsteady airfoil at U=17m/s (a) without control, (b) with pitching control gain, g_α=-0.25, δ_α=0.001, showing that before flutter speed the control decreases the vibrations.

IV. Conclusions

The results presented in this work enhance the scope and reliability of the aeroelastic analysis and design criteria of light and flexible wings. This simple and novel control strategy can supplement or replace conventional control devices, such as flaps and ailerons, with synthetic jet, or morphing type actuators to create a seamless aircraft with no moving control surfaces. For an airfoil in unsteady flow, the applied control was shown to both suppress the LCO, and extend the flutter boundary. The analysis performed in this paper can serve as guideline for selecting appropriate control gains and perturbation values to maximize performance. These results contribute, through control methodology, to the avoidance of design and operational pitfalls that may result in catastrophic failures, and can improve ride comfort. Our theory for nonlinear control will be readily reusable and capable of a broader envelope of design without weight penalties. Since the power required to implement this design is asymptotically zero, the actuators needed would be relatively simple. The uncomplicated form of our control plant promises affordable testing and later implementation.

V. Acknowledgments

Erik Bollt was supported for this work by the National Science Foundation under DMS-0404778. P. Marzocca would like to thank Prof. L. Librescu of Virginia Tech for his support, guidance and collaboration.

VI. References

[1] P. MARZOCCA, L. LIBRESCU, W.A. SILVA, "Aeroelastic Response of Nonlinear Wing Section by Functional Series

Technique," AIAA Journal, Vol. 40, No. 5, May 2002, pp. 813-824.

[2.] L. LIBRESCU, S. NA, P. MARZOCCA, C. CHUNG, and M.K. KWAK, "Active Aeroelastic Control of 2-D Wing-Flap Systems in an Incompressible Flowfield," AIAA Paper 2003-1414, 44th AIAA/ASME/ASCE/ASC Structures, Structural Dynamics, and Materials Conference, April 7-10, 2003, Norfolk, VA.

[3.] P. MARZOCCA, L. LIBRESCU, W.A. SILVA, "Flutter, Post-Flutter and Control of a Supersonic 2-D Lifting Surface," Journal of Guidance, Control, and Dynamics, Vol. 25, No. 5, September – October 2002, pp. 962-970.

[4.] L. LIBRESCU, G. CHIOCCHIA, P. MARZOCCA, "Implications of Cubic Physical / Aerodynamic Nonlinearities on the Character of the Flutter Instability Boundary," International Journal of Nonlinear Mechanics, Vol. 38, March 2003, pp. 173-199.

[5.] L. LIBRESCU, P. MARZOCCA, W.A. SILVA, "Post-Flutter Instability of a Shell Type Structures in Hypersonic Flow Field," Journal of Spacecraft and Rockets, Vol. 39, No. 5, September – October 2002, pp.802-812.

[6.] Z. QIN, P. MARZOCCA, L. LIBRESCU, "Aeroelastic Instability and Response of Advanced Aircraft Wings at Subsonic Flight Speeds," Aerospace Science and Technology, Vol. 6, No. 3, March 2002, pp. 195-208.

[7.] E.H. DOWELL, A Modern Course in Aeroelasticity, Sijthoff and Noordhoff, 1978.

[8.] E.H. DOWELL, J. EDWARDS, T.STRGNAC, "Nonlinear Aeroelasticity." Journal of Aircraft, Vol. 40, No. 5, 2003, pp. 857-874

[9.] B.H.K. LEE, S.J. PRICE, Y.S. WONG, "Nonlinear Aeroelastic Analysis of Airfoils: Bifurcation and Chaos," Progress in Aerospace Science, Vol. 35, 1999, pp 205-334.

[10.] D. BERGGREN, "Investigation of Limit Cycle Oscillations for a Wing Section with Nonlinear Stiffness," Aerospace Science and Technology. Vol. 8 27-34 (2004).

[11.] P. SHAHRZAD, M. MAHZOON "Limit Cycle Flutter of Airfoils in Steady and Unsteady Flows," Journal of Sound and Vibration. Vol. 256, No. 2 213-225 (2002).

[12.] B.D. COLLER, P.A. CHAMARA, "Structural Nonlinearities and the Nature of the Classic Flutter Instability," Journal of Sound and Vibration. Vol. 277, 711-739 (2004).

[13.] B.I. EPUREANU, L.S. TANG, M.P. PAÏDOUSSIS, "Coherent Structures and Their Influence on Dynamics of Aeroelastic Panels." International Journal of Non-Linear Mechanics, Vol. 39, 2004, pp 977-991.

[14.] S. TOUMIT, D.DARRACQ, "Simulation of Flutter Boundary and Hopf Bifurcation of a 2DOF Airfoil," ECCOMAS Paper, European Congress on Computational Methods in Applied Sciences and Engineering, September 11-14, 2000, Barcelona, Spain.

[15.] P.MARZOCCA, L.LIBRESCU, G. CHIOCCHIA, "Aeroelastic Response of 2-D Lifting Surfaces to Gust and Arbitrary Explosive Loading Signatures," International Journal of Impact Engineering, Vol. 25, 2001, pp 41-65.

[16.] V. MUKHOPADHYAY, "Historical Perspective on Analysis and Control of Aeroelastic Responses." Journal of Guidance, Control, and Dynamics, Vol. 26, 2003, pp 673-684.

[17.] H. HORIKAWA, E.H. DOWELL, "An Elementary Explanation of the Flutter Mechanism with Active Feedback Controls," Journal of Aircraft, Vol. 16, 1979, pp 225-232.

[18.] J.S. VIPPERMAN, R.L. CLARK, M.D. CONNER, E.H. DOWELL, "Investigation of the Experimental Active Control of a Typical Section Airfoil Using Trailing Edge Flap," Journal of Aircraft, Vol. 35, 1998, pp 224-229.

[19.] V. MUKHOPADHYAY, ED., "Benchmark Active Control Technology," Journal of Guidance, Control, and Dynamics, Part I Vol. 23, 2000, pp 913-960. Part II Vol. 23, 2000 pp 1093-1139. Part III Vol. 24, 2001, pp 146-192.

[20.] P. FRIEDMANN, D. GUILLOT, E. PRESENTE, "Adaptive Control of Aeroelastic Instabilities in Transonic Flow and its Scaling," Journal of Guidance, Control, and Dynamics, Vol. 20, 1997, pp. 1190- 1199.

[21.] R. LIND, M. BRENNER, Robust Aeroservoelastic Analysis. Springer-Verlag, Great Britain, 1999.

[22.] J.M. BARKER, G.J. BALAS, "Comparing Linear Parameter-Varying Gain-Scheduled Control Techniques for Active Flutter Suppression," Journal of Guidance, Control, and Dynamics, Vol. 23, No. 5, 2000, pp 948-955.

[23.] R.C. SCOTT, L.E. PADO, "Active Control of Wind-Tunnel Model Aeroelastic Response Using Neural Networks," Journal of Guidance, Control, and Dynamics, Vol. 2, No.6, 2000, pp 1100-1108.

[24.] D.M. GUILLOT, P.P. FRIEDMANN, "Fundamental Aeroservoelastic Study Combining Unsteady Computational Fluid Mechanics with Adaptive Control," Journal of Guidance, Control, and Dynamics. Vol. 23, No. 6, 2000, pp. 1117-1126.

[25.] J. KO, A.J. KURDILA, T.W. STRGANAC, "Nonlinear Control of a Prototypical Wing Section with Torsional Nonlinearity," Journal of Guidance, Control, and Dynamics, Vol. 20, No. 6, 1997, pp. 1181-1189.

[26.] R. ZHANG, S.N. SINGH, "Adaptive Output Feedback Control of an Aeroelastic System with Unstructured Uncertainties." Journal of Guidance, Control, and Dynamics. No. 3, 2001, pp 502- 509.

[27.] Y. ZENG, S.N. SINGH, "Output Feedback Variable Structure Adaptive Control of Aeroelastic Systems." Journal of Guidance, Control, and Dynamics, Vol. 21, No. 6, 1998, pp 830-837.

[28.] W. XING, S.N. SINGH, "Adaptive Output Feedback Control of a Nonlinear Aeroelastic Structure." Journal of Guidance, Control, and Dynamics. Col. 23, No. 6, 2000, pp. 1109-1116.

[29.] L.LIBRESCU, P. MARZOCCA, "Advances in the Linear/Nonlinear Control of Aeroelastic Structural Systems," Acta Mechanica (2005).

[30.] E. BOLLT, J.D. MEISS, "Targeting Chaotic Orbits to the Moon through Recurrence," Physics Letters A 204 373-378 (1995).

[31.] D. MORGAN, E. BOLLT, I. SCHWARTZ, "Computing constrained invariant sets," to appear Phys. Rev. E (2004).

[32.] N.J. CORRON, S.D.PETHEL, B.A. HOPPER, "Controlling Chaos with Simple Limiters." Physical Review Letters, Vol. 84, No. 17, 24 April 2000, pp 3835-3838.

[33.] Y.C. FUNG, An Introduction to the Theory of Aeroelasticity. New York: Dover Publications, 1969.

[34.] R.T. JONES, "The Unsteady Lift of a Wing of Finite Aspect Ratio," NACA Rept. 681 (1940).

[35] B.D. COLLER, P.A. CHAMARA, "Structural Nonlinearities and the Nature of the Classic Flutter Instability," Journal of Sound and Vibration. Vol. 277, 711-739 (2004).

[36] B.I. EPUREANU, L.S. TANG, M.P. PAïDOUSSIS, "Coherent Structures and Their Influence on Dynamics of Aeroelastic Panels." International Journal of Non-Linear Mechanics, Vol. 39, 2004, pp 977-991.

[37] S. TOUMIT, D.DARRACQ, "Simulation of Flutter Boundary and Hopf Bifurcation of a 2DOF Airfoil," ECCOMAS Paper, European Congress on Computational Methods in Applied Sciences and Engineering, September 11-14, 2000, Barcelona, Spain.